ATTENUATION OF INFRARED RADIATION WHEN PASSING THROUGH A WATER CURTAIN

Dalibor BALNER[1], Karla BARČOVÁ[2], Michal DOSTÁL[3]

Research article

Abstract: This article focuses on the interaction of infrared (IR) radiation with water droplets. The main objective of the article is the production of water mist in order of evaluation the reduction in intensity of IR radiation. In the experiments described in this paper, a set of five different nozzles was used with various spray characteristics. The respective nozzles were gradually located between the IR radiation source and a detector and the attenuation of IR radiation was assessed. The reduction in IR radiation intensity was determined and IR radiation transmittance was calculated for the respective tested nozzles.

Keywords: Infrared radiation, intensity, water curtain, water mist, droplet, nozzle.

Introduction

One of the areas of fire protection, in which water mist plays a key role, is the reduction in effects of thermal radiation during the heat transfer from a fire for the purpose of protection of intervening fire fighters or the limitation of fire propagation into other spaces. Thermal radiation is one of the three main principles of heat transfer, whereas creating a suitable water curtain can serve to attenuate radiation to the required level (in firefighting, as well as fire prevention). To optimize attenuation of thermal radiation it is necessary to create a water curtain of specific parameters, with respect to the conditions of the radiation source. This article focuses on the reduction in IR radiation intensity through a curtain of water mist, with respect to the defined intensity of radiation of the used radiation source, in three detected wavelength ranges. The article is the laboratory basis for the attenuation of IR radiation and can be used, amongst others, as a basis for a large-scale experiment.

Water curtains and their characteristics

- Increasing pressure/flow rate → production of finer droplets of a higher mass concentration → higher attenuation of radiation. (Cheung, 2009)
- With an increasing fire size, the attenuation of radiation also increases (Cheung, 2009)/ another source states that when a source radiates at lower temperatures (energy in longer wavelengths) there is easier attenuation. (Yang et al., 2003)
- With a decreasing nozzle diameter, the attenuation of radiation increases → production of finer droplets (3/8“ is better than 7/16“); Nozzle 3/8“ - approved by NFPA. (Cheung, 2009)
- They also have a significant cooling effect.
- The physical principle of water curtains is based on the absorption and scattering of radiation. (Cheung, 2009, Yang et al., 2003)
  - Droplets from several tens to several hundred μm have strong absorptive and anisotropic scattering characteristics, whereas water vapour and CO_2 only absorb radiation (depending on the wavelength). (Boulet et al., 2006)
- The maximum attenuation factor of radiation was achieved when the **radius** of droplets was approximately equal to IR - wavelength (0.6 - 25 μm) (Cheung, 2009, Ravigururajan et al., 1989)/ another source states that the spray provided maximum blocking efficiency when the droplet **diameter** was the same order as the maximum emission wavelength of the source. (Drysdale et al., 2000, Coppalle et al., 1993)

[1] VŠB - Technical University of Ostrava, Faculty of Safety Engineering, Ostrava, Czech Republic, dalibor.balner@vsb.cz

[2] VŠB - Technical University of Ostrava, Faculty of Safety Engineering, Ostrava, Czech Republic, karla.barcova@vsb.cz

[3] VŠB - Technical University of Ostrava, Faculty of Safety Engineering, Ostrava, Czech Republic, michal.dostal@vsb.cz

- An important role is played by the in-scattering of radiation (considering the two-dimensional/ two-flux model, not considering the Beer-Lambert Law). (Yang et al., 2003)

Therefore, the key parameters of water curtains are - droplet diameter, droplet mass concentration, molar fraction of gases (gases content), droplet falling rate, curtain thickness. (Coppalle et al., 1993, Cheung, 2009, Drysdale et al., 2000, Yang et al., 2003)

Material and methods

Production of water mist

In collaboration with PKS Servis spol. s r.o. (distributor and service centre for Tecnocooling products in Czech Republic, producer and seller of TechnoMIST equipment), for the purpose of producing water mist and subsequent evaluation the reduction in IR radiation intensity was used the device which the company offers primarily for cooling, humidification and reduction of dustiness of a specific environment. The equipment is comprised of a high-pressure water pump, piping system, fittings and nozzles of various flowrates (orifice sizes). A diagram of the measuring apparatus for the production of water mist is illustrated in Fig. 1.

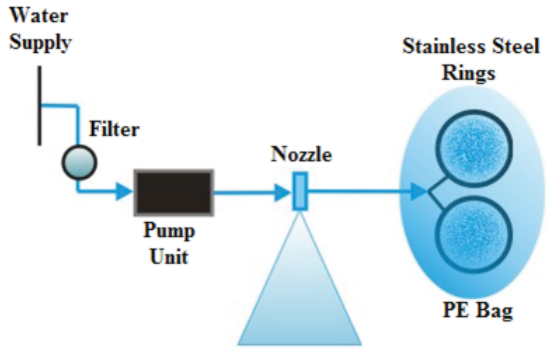

Fig. 1 Diagram of apparatus for the production of water mist

High-pressure water pump

A Tecnocooling high-pressure pump, type PREMIUM, is a plunger pump comprised of a brass head with three ceramic pistons, driven by a single-phase electromotor. The maximum operating pressure of the pump is 70 bars, at which the water flow rate at output from the pump is about 2 $l.min^{-1}$ (depending on the water quality). The pump´s industrial-grade electromotor is air cooled and has the following technical specifications: 230 V, 50 Hz, 1450 $ot.min^{-1}$ (RPM). The pump´s noise level is about 60 db (A). A standard water filter, with a plastic casing and cellulose cartridge, is fitted to the pump´s supply line as protection of the unit against the ingress of mechanical impurities into pistons and also as prevention of clogging of the fine nozzle heads. The filtration parameter for removing rough impurities is up to 5 µm. The pump with the supply line and filter is shown in Fig. 2.

Fig. 2 High-pressure pumping unit with supply line and filter

Piping system

The high-pressure piping system is comprised of black nylon hoses, 3/8" thick (5 mm inside diameter, 10 mm outside diameter, 2.5 mm wall thickness). The length of the hose from the pump to the first T-piece (measured nozzle) is 6.2 m and from the brass nozzle (T-piece) to the stainless-steel rings 5.2 m.

Fittings

At a distance of 6.2 m from the pump, the first T-piece (brass quick coupling for 3/8" hoses) is located, providing for the connection of the measured nozzle. From this T-piece, a hose continues for 5.2 m to the second T-piece, which provides for branching into two stainless steel rings with nozzles (the ring diameter is 40 cm and each ring contains 5 nozzles). Two stainless steel rings fitted with a total of 10 nozzles provide for the defined flow rate of the pump. The first ring is fitted with 100 µm, 150 µm, 200 µm, 300 µm and 500 µm nozzles, and the second stainless steel ring is fitted with 500 µm nozzles. To prevent excessive water mist from escaping into the surroundings and effecting measurement, the stainless steel rings with nozzles were placed into a PE bag (see Fig. 1). The branch to the measured nozzle contains the third T-piece used for connection of the pressure sensor which enables monitoring of pressure at the measured nozzle, and a 3/8" end nozzle holder. The tested nozzle can be changed on the end holder (100 µm, 150 µm, 200 µm, 300 µm and 500 µm). The pressure sensor is connected using a threaded set providing for transition from M20x1,5

DOI 10.1515/tvsbses-2017-0001

of the pressure sensor to the 3/8" nylon hose using a connector (gas taper ¼" to 3/8"). The stainless steel rings are also connected using a connector to a 3/8" hose. The first T-piece together with the branch to the measured nozzle and pressure sensor is shown in Fig. 3; the second T-piece and branching to the stainless steel rings with nozzles can be seen in Fig. 4.

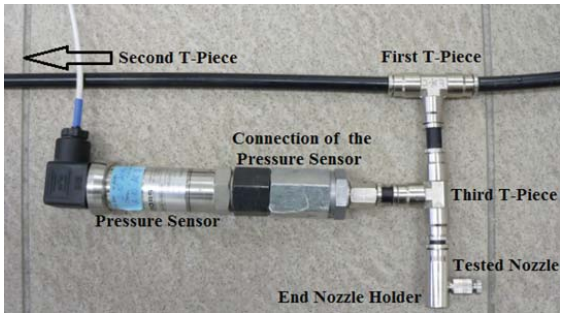

Fig. 3 Fittings 1

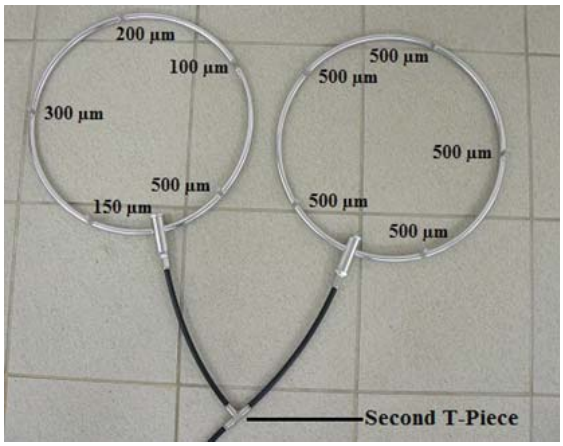

Fig. 4 Fittings 2

Nozzles

Measurement was done using nozzles with hole diameters of 100 µm, 150 µm, 200 µm, 300 µm and 500 µm. These tested nozzles ensured the production of water mist with various water droplet sizes and various mass concentrations. The respective nozzles differed also in water flow rate (Fig. 5) and spray cone width (Fig. 6). The 100 µm nozzle is not standardly supplied, however, it should have been marked 100 µm and the diameter of the hole should be smaller than nozzle 150 µm, according to available information. The flow rate measurement showed that this was not true, and it corresponds to a nozzle somewhere between 150 µm and 200 µm (the flow rate is closer to the nozzle 200 µm).

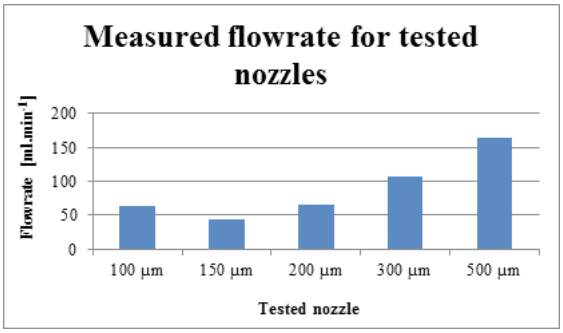

Fig. 5 Flow rates of tested nozzles

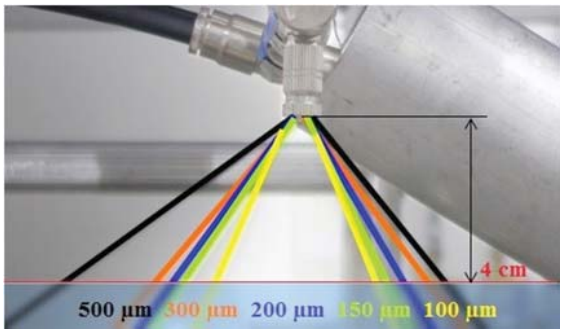

Fig. 6 Widths of spray cones of tested nozzles

Pressure sensor

The used pressure sensor from BD SENSORS s.r.o. was type DMP_333G-01, with a nominal range of 0 - 600 bars abs., and accuracy of 0.25 %. The pressure sensor calibration was valid for the duration of measurement. Display and recording of pressure was ensured by the ALMEMO® 2890-9 data logger from the German producer AHLBORN.

Reduction in intensity of IR radiation during passing through water mist curtain

Measuring of the reduction in infrared radiation intensity was done in laboratory conditions of the Faculty of Safety Engineering; the experimental apparatus is schematically depicted in Fig. 7. A Stabilized Tungsten IR Light Source (SLS202) was used as the radiation source, providing constant intensity of radiation of a black body at wavelength intervals from 0.45 to 5.5 µm.

The said wavelengths contain part of the visible spectrum and mainly the near infrared, short-wavelength infrared and mid-wavelength infrared radiation. Thorlabs (SLSC2) collimator optics was used to reduce the divergence of the radiation beam, which enabled a bigger distance between the radiation source and detector. Continual

radiation from the source had to be interrupted using a Standford research systems (SR540) optical chopper, with a frequency of $f = 320$ Hz, to provide for the subsequent processing of the signal. An IR lamp with collimator optics and used chopper are shown in Fig. 8.

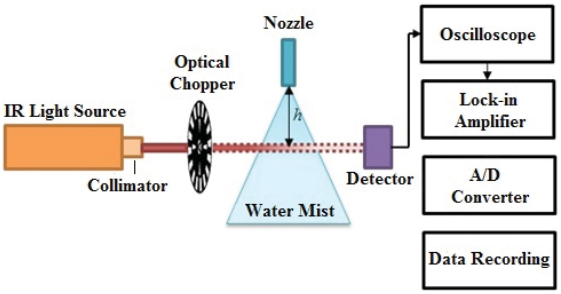

Fig. 7 Experimental apparatus diagram

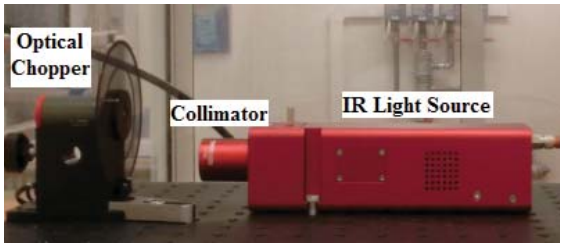

Fig. 8 IR radiation source, used optics and chopper

After passing of the radiation through the water curtain at a height of $h = 4$ cm under the water nozzle, the remaining radiation was detected using a light-sensitive detector. During measuring, three radiation detectors were used for various wavelength ranges: Thorlabs PDA20H-EC type PbSe detector, for wavelengths 1.5 - 4.8 µm, Thorlabs PDA30G-EC type PbS detector, for wavelengths 1 - 2.9 µm and Thorlabs PDA36A-EC type Si detector, for wavelengths 0.4 - 1.1 µm. Due to the high level of radiation, an optical iris had to be located in front of the PDA30G-EC sensor. No iris was used for the other detectors. The PDA30G-EC detector with optical iris is shown in Fig. 9. The emitted spectrum of the IR lamps and working range of the respective detectors with indicated relative sensitivities are shown in Fig. 10. The respective detectors do not demonstrate the same sensitivity across their whole ranges. The maximum sensitivity of the respective detectors is indicated in Fig. 10 by the darkest colour.

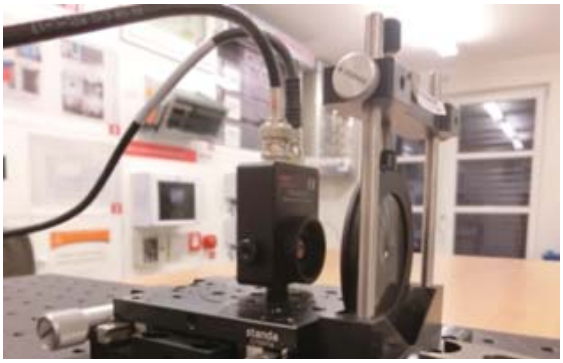

Fig. 9 IR radiation detector and used optical screen

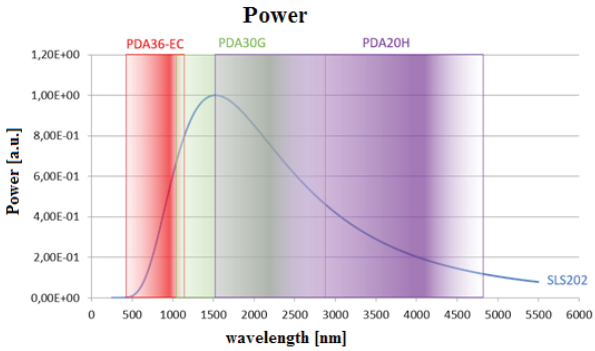

Fig. 10 Graph of lamp radiation intensity with marked detector ranges

Fig. 11 Shows the measuring apparatus setup for determining the reduction in IR radiation intensity.

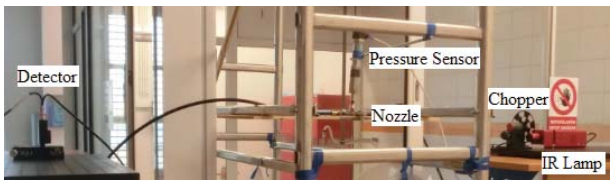

Fig. 11 Measuring apparatus

The following Fig. 12 shows the measuring apparatus with the nozzle switched on. In this Fig. 12, the scattering of radiation after passing through the water curtain can be seen clearly.

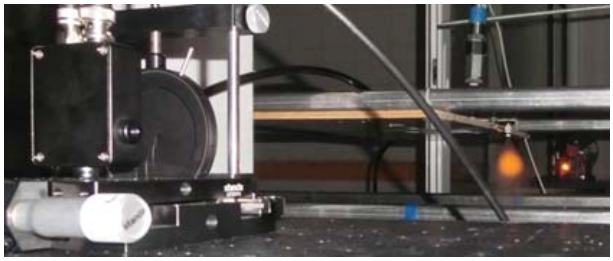

Fig. 12 Measuring apparatus with the nozzle switched on

The detail of scattering of radiation after passing through the water curtain is shown in Fig. 13.

Fig. 13 Detail of dispersed radiation on water droplets

A LeCroy waveSurfer 42Xs oscilloscope was used to display the output signal from the detector; this signal had a sinusoidal curve due to the modulation by the optical chopper. A Standford research systems SR830 DSP phase-sensitive amplifier was used to demodulate the signal from the detector, and the resultant signals, corresponding to values X and Y, were recorded in a computer using an analogue/digital converter, which was a Digilent (Analog discovery) oscilloscopic card in this case. Subsequently, it was necessary to calculate the resultant signal value in a table processor from these values according to formula (1).

$$R = \sqrt{X^2 + Y^2} \qquad (1)$$

The oscilloscope, phase-sensitive amplifier, Digilent oscilloscopic card and Almemo data logger with power supply (for recording the nozzle pressure) are shown in the following Fig. 14.

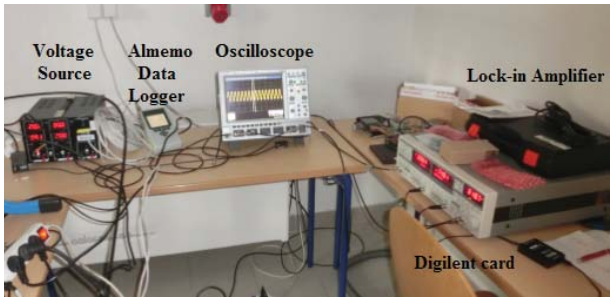

Fig. 14 Used experimental devices

Measuring procedure

The measurement of attenuation of infrared radiation through a water curtain, produced by tested nozzles, was conceived as follows. For a specific range of wavelengths, the IR radiation intensity incident on the detector was measured for the reference measurement and for the respective nozzles. A two-minute measuring time interval was chosen (depending on the accuracy of switching off the measurement recording). This time interval was selected as the most suitable for ensuring sufficient data of a specific measurement and monitoring (assessment) of changes in IR radiation intensity. First, the reference measurement - IR radiation intensity incident on the detector - was measured without application of water between the IR lamp and detector (no water curtain). Furthermore, the IR radiation intensity was determined while positioning a water curtain between the IR lamp and detector using the tested nozzles marked 100 µm, 150 µm, 200 µm, 300 µm and 500 µm. During the reference measurement, the maximum IR radiation intensity incident on the detector was determined, under the measuring conditions and with a specific measuring apparatus setup (see Fig. 15). After the performed reference, measuring was done with a specific tested nozzle. The respective nozzles were used to create a water curtain between the IR lamp and detector and the IR radiation, attenuated by passing through the water curtain, was recorded at 2-minute intervals. Five measurements were taken in each of the wavelength ranges, i.e. 0.4 - 1.1 µm, 1 - 2.9 µm a 1.5 - 4.8 µm (working ranges of the used detectors). In each measurement the reference value (no water curtain) was determined and reduction in IR radiation intensity was measured while applying the 100 µm, 150 µm, 200 µm, 300 µm and 500 µm nozzles. As was mentioned at the beginning of this chapter, the output signal from the detector had to be demodulated using a phase-sensitive amplifier and subsequently, using an oscilloscopic card, it was saved in the computer. The resultant signal value, calculated form formula (1), was expressed in the unit Volt. Therefore, the "relative IR radiation intensity", characterized by voltage, was assessed. From the measured voltage values, for the reference measurement and respective nozzles, it was possible to determine the reduction in the "IR radiation relative intensity" and define the IR radiation transmittance for the specific nozzle in the given wavelength range.

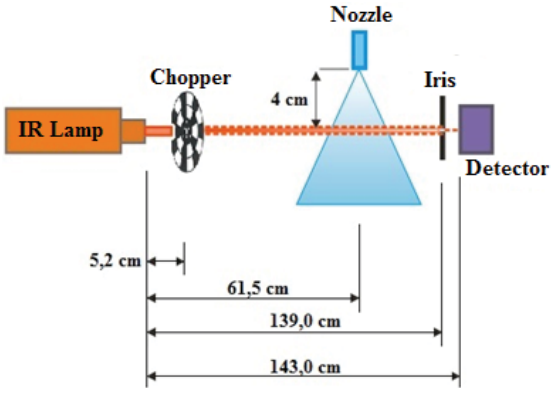

Fig. 15 Measuring apparatus specifications

DOI 10.1515/tvsbses-2017-0001

Results

Wavelength range 0.4 - 1.1 µm

This subchapter shows the evaluation of measured data for the detector working range 0.4 - 1.1 µm. These wavelengths include the areas of visible spectrum and near infrared radiation. The resultant transmittance values, for specific measurement and tested nozzles, are shown in Tab. 1 and Fig. 16.

Tab. 1 Transmittance of radiation in wavelength range 0.4 - 1.1 µm

	100 µm	150 µm	200 µm	300 µm	500 µm
Measurement 1 Transmittance [%]	65.02	65.87	60.11	61.87	51.72
Measurement 2 Transmittance [%]	65.85	65.65	60.19	62.21	52.24
Measurement 3 Transmittance [%]	65.62	65.56	60.41	62.25	51.14
Measurement 4 Transmittance [%]	65.71	65.53	60.16	62.20	54.26
Measurement 5 Transmittance [%]	66.11	65.98	60.20	62.83	51.83
Average Transmittance [%]	65.66	65.72	60.21	62.27	52.23

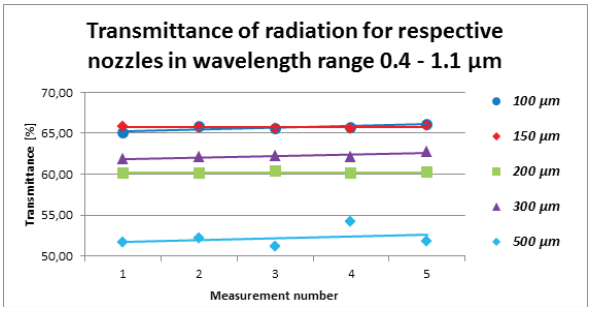

Fig. 16 Transmittance of radiation in wavelength range 0.4 - 1.1 µm

From the values shown in Tab. 1 and Fig. 16, it is clear that the highest attenuation of radiation was recorded for measurement with the 500 µm nozzle. This is followed by the 200 µm nozzle, which provides about a 2 % higher attenuation of radiation than the 300 µm nozzle, which is an interesting observation. This fact was most probably caused due to the smaller size of droplets for the 200 µm nozzle compared to the 300 µm nozzle, despite a lower flowrate. In the case of this wavelength range, the size of droplets made a more significant impact than the mass concentration. The 100 µm and 150 µm nozzles provide the highest radiation transmittance (the lowest attenuation). The transmittance values for these nozzles are almost identical in the respective measurements. The biggest difference in transmittance was seen in the given wavelength range between the 100 µm (150 µm) and 500 µm nozzles. Trend flowlines between the respective points were drawn for greater clarity of the graph.

Wavelength range 1.0 - 2.9 µm

The next measurement was done in the wavelength range 1.0 - 2.9 µm. This subchapter focuses on evaluation of measured data in this interval. The wavelengths include near infrared and short-wavelength infrared radiation.

The resultant transmittance values, for specific measurement and tested nozzles, are shown in Tab. 2 and Fig. 17:

Tab. 2 Transmittance of radiation in wavelength range 1.0 - 2.9 µm

	100 µm	150 µm	200 µm	300 µm	500 µm
Measurement 1 Transmittance [%]	66.26	67.46	58.51	62.96	53.75
Measurement 2 Transmittance [%]	67.33	67.88	59.42	63.74	54.57
Measurement 3 Transmittance [%]	66.76	67.57	59.28	63.01	53.40
Measurement 4 Transmittance [%]	66.38	66.92	58.80	63.07	51.55
Measurement 5 Transmittance [%]	66.65	67.48	58.70	63.45	52.10
Average Transmittance [%]	66.67	67.46	58.94	63.25	53.07

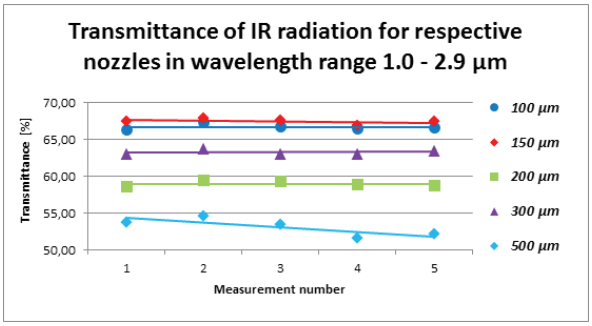

Fig. 17 Transmittance of radiation in wavelength range 1.0 - 2.9 µm

From the values shown in Tab. 2 and Fig. 17, it is clear that the highest attenuation of radiation was recorded for measurement with the 500 µm nozzle. This is followed by the 200 µm and 300 µm nozzles with an average difference in transmittance

of 4.31 % between these nozzles. The 100 µm and 150 µm nozzles provide the lowest attenuation of IR radiation. The biggest difference in transmittance was seen in the given wavelength range between the 500 µm and 150 µm nozzles. Trend flowlines between the respective points were drawn for greater clarity of the graph, just as in the previous case.

Wavelength range 1.5 - 4.8 µm

The third measurement of the reduction in IR radiation intensity was done in the wavelength range 1.5 - 4.8 µm. This section shows the evaluation of measured data for respective nozzles in the given spectrum, which primarily includes short-wavelength infrared and mid-wavelength infrared radiation.

The resultant transmittance values, for specific measurement and tested nozzles, are shown in Tab. 3 and Fig. 18:

Tab. 3 Transmittance of radiation in wavelength range 1.5 - 4.8 µm

	100 µm	150 µm	200 µm	300 µm	500 µm
Measurement 1 Transmittance [%]	60.08	59.49	51.57	54.19	39.86
Measurement 2 Transmittance [%]	59.74	59.33	51.61	53.98	42.24
Measurement 3 Transmittance [%]	60.46	60.33	51.97	55.12	42.61
Measurement 4 Transmittance [%]	59.84	59.88	51.78	54.28	42.13
Measurement 5 Transmittance [%]	60.95	61.45	52.02	55.88	41.28
Average Transmittance [%]	60.21	60.10	51.79	54.69	41.62

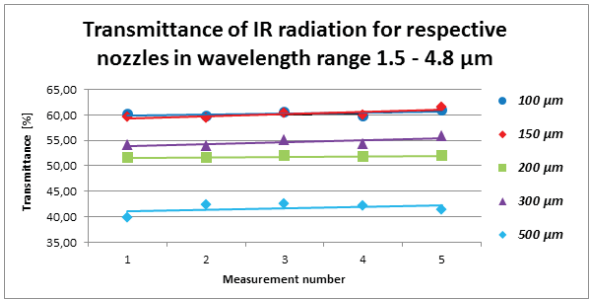

Fig. 18 Transmittance of radiation in wavelength range 1.5 - 4.8 µm

As in the case of previous wavelength ranges, also in the 1.5 - 4.8 µm range the highest attenuation of IR radiation was recorded for the 500 µm nozzle, see Tab. 3 and Fig. 18. The next in line is the 200 µm nozzle, which caused better attenuation of IR radiation for the given wavelength range than the 300 µm nozzle (difference of 2.9 % between nozzles). The lowest attenuation of IR radiation was provided, as in the previous cases, by the 100 µm and 150 µm nozzles. The values for these two nozzles correlate closely, as can be seen in Fig. 18. Fig. 18 also clearly shows that the biggest difference in terms of IR radiation attenuation, for the given spectrum, was between the 100 µm (150 µm) and 500 µm nozzles. The difference between the nozzles is 18.59 ± 0.79 %, δ_t = 5.84 %. Trend flowlines between the respective points were drawn for greater clarity of the graph, just as in the previous cases.

Conclusion

The key parameters of water mist effecting the reduction in IR radiation intensity are mass concentration of droplets and their size. A change of these parameters was achieved by nozzles with different orifice. The increasing size of the nozzle orifice led to an increase in water flowrate, as well as the width of the spray cone (in most cases). The highest water flow rate and widest spray cone for the 500 µm nozzle provided the highest attenuation of radiation in all tested wavelength ranges. This was followed by the 200 µm nozzle, which provided a higher reduction in radiation intensity than the 300 µm nozzle in all tested ranges. This fact was most probably caused by the smaller droplet size of the 200 µm nozzle compared to the 300 µm nozzle, despite the lower water flow rate and narrower spray cone. In these wavelength ranges the droplet size most likely had a greater effect than the mass concentration. The lowest radiation attenuation in all tested ranges was recorded for the 100 m and 150 µm nozzles. These nozzles had the lowest flow rate and narrowest spray cone.

Acknowledgement

The development of the aforementioned charges was possible thanks to project no. VI 20152019047, entitled: "Development of the rescue destructive bombs for the disposal of statically damaged buildings", which was approved and implemented under the Security Research Programme of the Ministry of Interior of the Czech Republic BV III/1-VS.

References

Boulet, P., Collin, A., Parent, G. 2006. Heat transfer through a water spray curtain under the effect of a strong radiative source. *Fire Safety Journal*. 41(1): 15-30. DOI: 10.1016/j.firesaf.2005.07.007.

Cheung, W.Y. 2009. *Radiation blockage of water curtains* [online]. [cit. 2014-09-30]. Available at: http://www.bse.polyu.edu.hk/researchCentre/Fire_Engineering/summary_of_output/journal/IJEPBFC/2009/P7-13.pdf.

Coppalle, A., Nedelka, D., Bauer, B. 1993. Fire protection: Water curtains. *Fire Safety Journal*. 20 (3): 241-255. DOI: 10.1016/0379-7112(93)90046-S. Available at: http://linkinghub.elsevier.com/retrieve/pii/037971129390046S.

Drysdale, D., Grant, G., Brenton, J. 2000. Fire suppression by water sprays. *Progress in Energy and Combustion Science*. 26 (2): 52. DOI: 10.1016/S0360-1285(99)00012-X. Available at: http://www.sciencedirect.com/science/article/pii/S036012859900012X#.

Ravigururajan, T. S., Beltran, M. R. 1989. A Model for Attenuation of Fire Radiation Through Water Droplets. In *Fire Safety Journal*. Elsevier Science Publishers Ltd, England. Available at: http://www.sciencedirect.com/science/article/pii/0379711289900027.

Yang, W., Parker, T., Ladouceur, H.D., Kee, R. J. 2003. The interaction of thermal radiation and water mist in fire suppression. *Fire Safety Journal*. Elsevier Ltd. Available at: http://www.sciencedirect.com/science/article/pii/S0379711203000948.